A Nonsymmetric Compliance Matrix Approach to Nonlinear Multimodulus Orthotropic Materials

Robert M. Jones*
Southern Methodist University, Dallas, Texas

Multimodulus materials have moduli or stiffnesses under tension loading which are different from those under compression loading. Several approaches to their analysis have been suggested recently. Most of these approaches are based on the hypothesis that the compliance matrix in the strain-stress relations must be symmetric. Jones makes the matrix symmetric by weighting the tension compliances and the compression compliances on the basis of the proportion of tensile and compressive stresses. Isabekyan and Khachatryan determine very severe restrictions under which a multimodulus material has a symmetric compliance matrix in all coordinate systems. However, the Jones weighted compliance matrix approach cannot be derived from basic principles. Moreover, the Isabekyan and Khachatryan restricted compliance matrix approach is not realistic because the properties of known multimodulus materials do not satisfy their restrictions. The purpose of this paper is to relax the previously held requirement of compliance matrix symmetry to see whether suitable agreement can be obtained between predicted and measured strain response of ATJ-S graphite to mixed tension and compression loading under plane stress conditions.

Nomenclature

$E_c(E_t)$ = Young's modulus in compression (tension), Fig. 1
E^{45}_{mn} = Young's modulus at 45° to principal material directions
G_{mn} = shearing modulus in the principal material directions
S_{ij} = compliances in strain-stress relations [Eq. (1)]
ν_{mn} = Poisson's ratio for contraction (expansion) in the n direction due to extension (compression) in the m direction

Subscripts

c = compression
m,n = principal material directions
p,q = principal stress directions
t = tension
tc = abbreviation for tension or compression, as appropriate

Superscripts

mn = principal material coordinates
pq = principal stress coordinates
xy = arbitrary coordinates at angle ω from principal stress coordinates, Fig. 2
45 = at 45° to principal material directions

Introduction

FIBER-REINFORCED composite materials are used in a wide variety of applications ranging from laminated aircraft wings to golf club shafts. Granular composite materials are used in re-entry vehicle nosetips, nuclear reactor control rods, etc. In the current energy crisis, accurate stress analysis of reactor control rods is essential to understand their behavior in order to prevent failures. Otherwise, further repetition of control rod failures with subsequent reactor shutdowns will prevent nuclear energy sources from attaining their obviously needed potential. Accurate stress analysis is no less essential in most other applications of composite materials.

Received Feb. 14, 1977; revision received June 3, 1977.
Index categories: Materials, Properties of; Structural Composite Materials; Structural Statics.

*Professor of Solid Mechanics; also Consultant, Lockheed Missiles and Space Company, Inc., Sunnyvale, Calif. Associate Fellow AIAA.

One of the important characteristics of composite materials is that they often exhibit moduli or stiffnesses under tension loading which are different from those under compression loading. Such materials are called multimodulus materials, and their uniaxial stress-strain behavior is represented schematically in Fig. 1. There, a nonlinear transition region might exist between fairly linear tension and compression portions of the curve. Moreover, the stress-strain behavior at high stress levels is often quite nonlinear. The actual nonlinear behavior often is replaced with a bilinear model as in Fig. 1 as a first-order approximation of the actual behavior. We shall investigate a higher-order approximation of the nonlinear behavior in our pursuit of how best to analyze multimodulus materials.

Jones gives examples of multimodulus granular and fiber-reinforced composite materials.[1] For both classes of materials, he observes that sometimes the tension modulus is larger than the compression modulus, and sometimes the reverse is true. We recognize that such perhaps inconsistent characteristics exist and proceed to model the apparent physical behavior rather than to attempt to explain the curious nature of the behavior.

Given that the multimodulus stress-strain behavior can be modeled with a linear or nonlinear model, the definition remains of the actual multiaxial stress-strain or constitutive relations that are required in stress analysis. Over the past decade, Ambartsumyan and his associates,[2-6] in the process of analyzing stresses in shells and bodies of revolution, defined a set of stress-strain relations which are referred to herein as the Ambartsumyan material model. The Ambartsumyan model

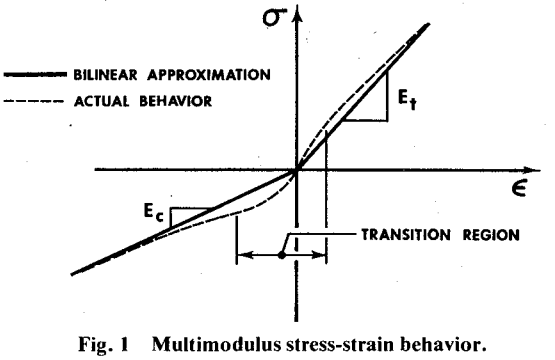

Fig. 1 Multimodulus stress-strain behavior.

for orthotropic multimodulus materials has a nonsymmetric compliance matrix (the set of coefficients of the stresses in a matrix strain-stress relation). Isabekyan and Khachatryan[7] determine very severe restrictions on material properties under which a multimodulus material has a symmetric compliance matrix in all coordinate systems. However, their restrictions are not satisfied for known multimodulus materials. Jones[1] makes the compliance matrix symmetric by weighting the tension compliances and the compression compliances on the basis of the proportions of tensile and compressive stresses in the directions affecting the otherwise unequal cross-compliances (off-diagonal terms in the compliance matrix). However, Jones uses a compliance weighting procedure that, although it may be an effective engineering approximation to the multimodulus stress analysis problem, cannot be derived from basic principles. Specifically, the weighting expression is selected arbitrarily but apparently in consonance with known physical principles.

The objective of this paper is to re-examine the compliance matrix symmetry or nonsymmetry question by comparing predicted with measured strain response to mixed tension and compression loading under plane stress conditions. This comparison is performed for ATJ-S graphite, which is a fairly well-characterized transversely isotropic multimodulus granular composite material with nonlinear stress-strain behavior. First, the plane stress material model is described for linear elastic multimodulus materials. Then, the elastic analysis is modified to account for stress-strain curve nonlinearities in the manner of Jones and Nelson.[8-11] Specifically, the mechanical properties in tension and in compression are expressed in terms of the strain energy of an equivalent elastic system. Then, in accordance with the Jones-Nelson nonlinear material model, we iterate to find the degree of nonlinearity for which the calculated strain energy of deformation is consistent with strain energy used to find the mechanical properties.

At this point, an apparent inconsistency arises because the concept of strain energy ordinarily is not associated with the concept of nonconservative material behavior (because of compliance matrix asymmetry). That is, a strain energy function does not exist for nonconservative mechanical systems. However, the strain energy in the Jones-Nelson material model is used only to determine the degree of nonlinearity in a deformation theorh of plasticity. Thus, we cannot analyze nonproportional loading situations anyway. The actual solution of the nonsymmetric equilibrium equations is performed with an equation solver for nonsymmetric matrix equations. Thus, the apparent inconsistency is, in fact, acceptable.

Finally, we compare our strain predictions with strains measured by Jortner[12-14] for a hollow tubular body under axial compression and circumferential tension. The gage section of the body where strains are measured is under essentially plane stress conditions, as confirmed with a finite element analysis. Thus, we need not bother to perform a more geometrically correct analysis. This comparison is the simplest that can be made with presently available data. Moreover, the strain measurements were performed carefully, so that the potential exists for investigating a very sensitive issue in the analysis of multimodulus materials.

Linear Multimodulus Material Model

A material model is defined with its stress-strain relations or strain-stress relations. The Ambartsumyan strain-stress relations in principal stress (p-q) coordinates for an orthotropic material under plane stress are[6]

$$\epsilon_p = S_{11}^{pq}\sigma_p + S_{12}^{pq}\sigma_q \tag{1a}$$

$$\epsilon_q = S_{21}^{pq}\sigma_p + S_{22}^{pq}\sigma_q \tag{1b}$$

$$\gamma_{pq} = S_{61}^{pq}\sigma_p + S_{y2}^{pq}\sigma_q \tag{1c}$$

Note that principal strain directions do not coincide with principal stress directions, since $\gamma_{pq} \neq 0$. Moreover, in other theories, the values of S_{12}^{pq} and S_{21}^{pq} are chosen so that these two cross-compliances are equal, i.e., so that the compliance matrix is symmetric.[1,7] However, we drop the requirement of symmetry and allow $S_{12}^{pq} \neq S_{21}^{pq}$. Thus, Eq. (1) is effectively a representation of an anisotropic material (because of the S_{61}^{pq} and S_{62}^{pq} terms) with a nonsymmetric compliance matrix.

The compliances in principal stress (p-q) coordinates, i.e., the S_{ij}^{pq}, take on different values depending on the signs of the principal stresses according to

$$\text{if } \sigma_p > 0 \text{ and } \sigma_q > 0;\ S_{ij}^{pq} = S_{ij_t}^{pq} \tag{2a}$$

$$\text{if } \sigma_p < 0 \text{ and } \sigma_q < 0;\ S_{ij}^{pq} = S_{ij_c}^{pq} \tag{2b}$$

$$\text{if } \sigma_p > 0 \text{ and } \sigma_q < 0;\ S_{11_t}^{pq},\ S_{12_c}^{pq},\ S_{21_t}^{pq},\ S_{22_c}^{pq},\ S_{61_t}^{pq},\ S_{62_c}^{pq} \tag{2c}$$

$$\text{if } \sigma_p < 0 \text{ and } \sigma_q > 0;\ S_{11_c}^{pq},\ S_{12_t}^{pq},\ S_{21_c}^{pq},\ S_{22_t}^{pq},\ S_{61_c}^{pq},\ S_{62_t}^{pq} \tag{2d}$$

The tension and compression compliances in principal stress ($p-q$) coordinates, i.e., the $S_{ij_t}^{pq}$ and $S_{ij_c}^{pq}$, are related to the tension and compression compliances in principal material (m-n) coordinates, i.e., the $S_{ij_t}^{mn}$ and $S_{ij_c}^{mn}$, respectively, by the usual transformations of anisotropic elasticity[15]:

$$S_{11_{tc}}^{pq} = S_{11_{tc}}^{mn}\cos^4\beta + (2S_{12_{tc}}^{mn} + S_{66_{tc}}^{mn})\sin^2\beta\cos^2\beta + S_{22_{tc}}^{mn}\sin^4\beta \tag{3a}$$

$$S_{12_{tc}}^{pq} = S_{12_{tc}}^{mn} + (S_{11_{tc}}^{mn} + S_{22_{tc}}^{mn} - 2S_{12_{tc}}^{mn} - S_{66_{tc}}^{mn})\sin^2\beta\cos^2\beta \tag{3b}$$

$$S_{21_{tc}}^{pq} = S_{12_{tc}}^{mn} + (S_{11_{tc}}^{mn} + S_{22_{tc}}^{mn} - 2S_{12_{tc}}^{mn} - S_{66_{tc}}^{mn})\sin^2\beta\cos^2\beta \tag{3c}$$

$$S_{22_{tc}}^{pq} = S_{11_{tc}}^{mn}\sin^4\beta + (2S_{12_{tc}}^{mn} + S_{66_{tc}}^{mn})\sin^2\beta\cos^2\beta + S_{22_{tc}}^{mn}\cos^4\beta \tag{3d}$$

$$S_{61_{tc}}^{pq} = [S_{22_{tc}}^{mn}\sin^2\beta - S_{11_{tc}}^{mn}\cos^2\beta + \tfrac{1}{2}(2S_{12_{tc}}^{mn} + S_{66_{tc}}^{mn})\cos 2\beta]\sin 2\beta \tag{3e}$$

$$S_{62_{tc}}^{pq} = [S_{22_{tc}}^{mn}\cos^2\beta - S_{11_{tc}}^{mn}\sin^2\beta - \tfrac{1}{2}(2S_{12_{tc}}^{mn} + S_{66_{tc}}^{mn})\cos 2\beta]\sin 2\beta \tag{3f}$$

where the subscript tc is used to denote t or c, as appropriate, and β is the angle between principal stress (p-q) directions and principal material (m-n) directions, as in Fig. 2. Note that the usual symmetry of compliances in pure tension and in pure compression is preserved, i.e., $S_{12_t} = S_{21_t}$ and $S_{12_c} = S_{21_c}$. Thus, the expression for $S_{21_{tc}}^{pq}$ is identical to that for $S_{12_{tc}}^{pq}$ in pure tension or pure compression. However, in states of mixed tension and compression, $S_{12_{tc}}^{pq} \neq S_{21_{tc}}^{pq}$. The compliances

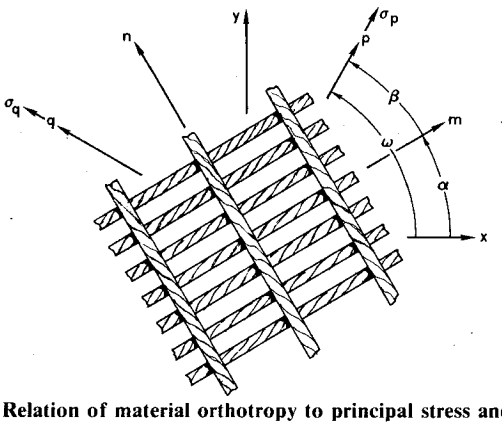

Fig. 2 Relation of material orthotropy to principal stress and body coordinates.

in principal material coordinates, i.e., the $S^{mn}_{ij_{tc}}$, are related to the usual engineering constants by

$$S^{mn}_{11_{tc}} = 1/E_{m_{tc}};\quad S^{mn}_{22_{tc}} = 1/E_{n_{tc}};\quad S^{mn}_{66_{tc}} = 1/G_{mn_{tc}} \tag{4a}$$

$$S^{mn}_{12_{tc}} = -\nu_{mn_{tc}}/E_{m_{tc}} = -\nu_{nm_{tc}}/E_{n_{tc}} \tag{4b}$$

where $\nu_{mn_t} = -\epsilon_n/\epsilon_m$ for $\sigma_m = \sigma_t$ and all other stresses are zero. There are eight independent material properties in Eq. (4): four in tension and four in compression.

Note that the usual reciprocal relations are assumed in Eq. (4) to be valid in both all-tension and all-compression stress states, i.e.,

$$\nu_{mn}/E_m = \nu_{nm}/E_n \tag{5}$$

where the applied uniaxial stress is either tension or compression. This assumption or hypothesis has not been verified by precise measurement for multimodulus materials. The validity of this hypothesis is questioned because Poisson's ratio determinations involve either a tensile normal stress and a transverse contraction or a compressive normal stress and a transverse extension. Thus, a state of mixed tension (stress) and compression (strain) or of mixed compression (stress) and tension (strain), respectively, exists.

Similarly, shear moduli are usually measured in a state of pure shear which is inherently a state of mixed tension and compression wherein one principal stress is tension and the other is compression. However, G_{mn_t} and G_{mn_c} in Eq. (4) are defined only in pure tension and pure compression, respectively. Therefore, these shear moduli cannot be measured in a shear test. Instead, in accordance with a suggestion by Tsai,[16] the tension modulus at 45° to the principal material axes, $E^{45}_{mn_t}$, is measured, whereupon

$$S^{mn}_{66_t} = \frac{1}{G_{mn_t}} = \frac{4}{E^{45}_{mn_t}} - \left(\frac{1}{E_{m_t}} + \frac{1}{E_{n_t}} - \frac{2\nu_{mn_t}}{E_{m_t}}\right) \tag{6}$$

which is derived from a simple transformation of compliances. Similarly,

$$S^{mn}_{66_c} = \frac{1}{G_{mn_c}} = \frac{4}{E^{45}_{mn_c}} - \left(\frac{1}{E_{m_c}} + \frac{1}{E_{n_c}} - \frac{2\nu_{mn_c}}{E_{m_c}}\right) \tag{7}$$

The G_{mn} measured in a shear test can be shown to be the average of the indirectly evaluated G_{mn_t} and G_{mn_c}. This theoretical contention can be verified in principle by measuring G_{mn} in addition to the principal material properties, including $E^{45}_{mn_t}$ and $E^{45}_{mn_c}$, and then comparing the measured G_{mn} with the calculated G_{mn}. The qualifier "in principle" is appropriate because good shear measurements are very difficult to make to the level necessary to perform the foregoing comparison with accuracy sufficient to draw a definitive conclusion.

In arbitrary body (x-y) coordinates oriented at angle ω to the principal stress coordinates as in Fig. 2, the compliances S^{ij}_{xy} are obtained from the compliances in principal stress directions, i.e., the S^{pq}_{ij}, by use of the transformations[6]

$$S^{xy}_{11} = S^{pq}_{11}\cos^4\omega + (S^{pq}_{21} + S^{pq}_{12})\sin^2\omega\cos^2\omega + S^{pq}_{22}\sin^4\omega - \tfrac{1}{2}(S^{pq}_{61}\cos^2\omega + S^{pq}_{62}\sin^2\omega)\sin 2\omega \tag{8a}$$

$$S^{xy}_{12} = (S^{pq}_{11} + S^{pq}_{22})\sin^2\omega\cos^2\omega + S^{pq}_{21}\sin^4\omega + S^{pq}_{12}\cos^4\omega - \tfrac{1}{2}(S^{pq}_{61}\sin^2\omega + S^{pq}_{62}\cos^2\omega)\sin 2\omega \tag{8b}$$

$$S^{xy}_{16} = [\tfrac{1}{2}(S^{pq}_{62} - S^{pq}_{61})\sin 2\omega + (S^{pq}_{11} - S^{pq}_{12})\cos^2\omega - (S^{pq}_{22} - S^{pq}_{21})\sin^2\omega]\sin 2\omega \tag{8c}$$

$$S^{xy}_{22} = S^{pq}_{22}\cos^4\omega + (S^{pq}_{12} + S^{pq}_{21})\sin^2\omega\cos^2\omega + S^{pq}_{11}\sin^4\omega + \tfrac{1}{2}(S^{pq}_{62}\cos^2\omega + S^{pq}_{61}\sin^2\omega)\sin 2\omega \tag{8d}$$

$$S^{xy}_{21} = (S^{pq}_{22} + S^{pq}_{11})\sin^2\omega\cos^2\omega + S^{pq}_{12}\sin^4\omega + S^{pq}_{21}\cos^4\omega + \tfrac{1}{2}(S^{pq}_{62}\sin^2\omega + S^{pq}_{61}\cos^2\omega)\sin 2\omega \tag{8e}$$

$$S^{xy}_{26} = [\tfrac{1}{2}(S^{pq}_{61} - S^{pq}_{62})\sin 2\omega - (S^{pq}_{22} - S^{pq}_{21})\cos^2\omega + (S^{pq}_{11} - S^{pq}_{12})\sin^2\omega]\sin 2\omega \tag{8f}$$

$$S^{xy}_{61} = S^{pq}_{61}\cos^4\omega - S^{pq}_{62}\sin^4\omega - (S^{pq}_{61} - S^{pq}_{62})\sin^2\omega\cos^2\omega + [(S^{pq}_{11} - S^{pq}_{21})\cos^2\omega - (S^{pq}_{22} - S^{pq}_{12})\sin^2\omega]\sin 2\omega \tag{8g}$$

$$S^{xy}_{62} = S^{pq}_{62}\cos^4\omega - S^{pq}_{61}\sin^4\omega - (S^{pq}_{62} - S^{pq}_{61})\sin^2\omega\cos^2\omega - [(S^{pq}_{22} - S^{pq}_{12})\cos^2\omega - (S^{pq}_{11} - S^{pq}_{21})\sin^2\omega]\sin 2\omega \tag{8h}$$

$$S^{xy}_{66} = [(S^{pq}_{11} + S^{pq}_{22} - S^{pq}_{21} - S^{pq}_{12})\sin 2\omega + (S^{pq}_{61} - S^{pq}_{62})(\cos^2\omega - \sin^2\omega)]\sin 2\omega \tag{8i}$$

The compliances S^{pq}_{16}, S^{pq}_{26}, and S^{pq}_{66} do not appear in Eq. (8) because they do not exist in principal stress coordinates and do not affect the strains in arbitrary x-y coordinates. Moreover, the compliances S^{xy}_{ij} do not reduce to the transformed compliances for symmetric anisotropic materials even when $S^{pq}_{12} = S^{pq}_{21}$ because S^{pq}_{16}, S^{pq}_{26}, and S^{pq}_{66} are absent. Basically, the S^{xy}_{ij} constitute a nonsymmetric compliance matrix in arbitrary x-y coordinates:

$$\begin{Bmatrix} \epsilon_x \\ \epsilon_y \\ \gamma_{xy} \end{Bmatrix} = \begin{bmatrix} S^{xy}_{11} & S^{xy}_{12} & S^{xy}_{16} \\ S^{xy}_{21} & S^{xy}_{22} & S^{xy}_{26} \\ S^{xy}_{61} & S^{xy}_{62} & S^{xy}_{66} \end{bmatrix} \begin{Bmatrix} \sigma_x \\ \sigma_y \\ \tau_{xy} \end{Bmatrix} \tag{9}$$

Predictions of strains in linear multimodulus materials under biaxial mixed tension and compression loading are possible with Eqs. (1-9). However, known multimodulus materials have nonlinear stress-strain behavior, and so the linear multimodulus theory cannot be verified. Thus, we must develop a suitable nonlinear multimodulus theory before we can compare predicted and measured strain response.

The Ambartsumyan material model can be shown to have different shear moduli when a "positive" shear stress at 45° to principal material directions is applied than when a "negative" shear stress is applied, as in Fig. 3. This behavior is apparently in accordance with the known fact that composite material shear strengths are different under those conditions.[17] However, part of the reason that the strengths are different must be assumed to be the same reason that the stiffnesses or moduli are different. To demonstrate that the

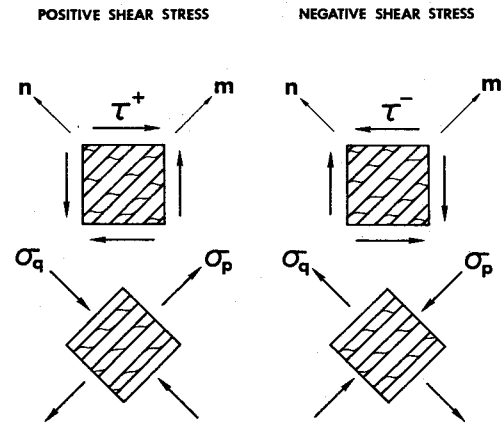

Fig. 3 Positive and negative shear stress at 45° to principal material directions.

Ambartsumyan material model does indeed exhibit this behavior, consider the cases of "positive" and "negative" shear stress at 45° to principal material directions in Fig. 3. The compliances in principal stress coordinates for the "positive" shear stress case are

$$S_{11}^{pq} = S_{11_t}^{mn}; \quad S_{12}^{pq} = S_{12_c}^{mn}; \quad S_{21}^{pq} = S_{21_t}^{mn} \tag{10a}$$

$$S_{22}^{pq} = S_{22_c}^{mn}; \quad S_{61}^{pq} = 0; \quad S_{62}^{pq} = 0 \tag{10b}$$

At 45° to the principal stress and principal material coordinates, pure shear stress exists, and, from Eq. (8),

$$S_{66}^{45} = S_{11}^{pq} + S_{22}^{pq} - S_{21}^{pq} - S_{12}^{pq} \tag{11}$$

The shear modulus is the inverse of S_{66}^{45} and can be expressed in terms of the S_{ij}^{mn} for "positive" shear stress through use of Eq. (10) as

$$G_t^{45} = 1/(S_{11_t}^{mn} + S_{22_c}^{mn} - S_{21_t}^{mn} - S_{12_c}^{mn}) \tag{12}$$

The compliances in principal stress coordinates for the "negative" shear stress case are

$$S_{11}^{pq} = S_{11_c}^{mn}; \quad S_{12}^{pq} = S_{12_t}^{mn}; \quad S_{21}^{pq} = S_{21_c}^{mn} \tag{13a}$$

$$S_{22}^{pq} = S_{22_t}^{mn}; \quad S_{61}^{pq} = 0; \quad S_{62}^{pq} = 0 \tag{13b}$$

Thus, upon substitution of Eq. (13) in Eq. (11),

$$G_c^{45} = 1/(S_{11_c}^{mn} + S_{22_t}^{mn} - S_{21_c}^{mn} - S_{12_t}^{mn}) \tag{14}$$

Finally, upon comparison of G_t^{45} with G_c^{45}, we see that the shear moduli are obviously different when the sign of the shear stress is reversed in coordinates at 45° to principal material directions. Reversing the sign of the shear stress in principal material directions is easily shown to result in the same shear moduli.[1]

Nonlinear Multimodulus Material Model

We adapt the Jones-Nelson nonlinear multimodulus material model for symmetric compliance matrices[10] to the present nonsymmetric compliance matrix situation. First, we display the essence of the Jones-Nelson model for symmetric compliance matrices. Then, we describe the associated iteration procedure to account for a nonsymmetric compliance matrix. Finally, we discuss three possible strain energy functions for use in the nonlinear multimodulus nonsymmetric compliance matrix material model.

Jones-Nelson Nonlinear Multimodulus Material Model for Symmetric Compliance Matrices

In the Jones-Nelson model,[10] we express all independent nonlinear mechanical properties for an orthotropic material under plane stress ($E_{m_{tc}}$, $E_{n_{tc}}$, $\nu_{mn_{tc}}$, and $E_{mn_{tc}}^{45}$) in terms of the strain energy of an equivalent linear elastic mechanical system:

$$\text{mechanical property}_i = A_i[1 - B_i(U/U_{0_i})^{C_i}] \tag{15}$$

where i is the property number (ranging from 1 to 8), A is the initial elastic modulus, B the initial curvature, and C the rate of change of curvature of the stress-strain curve; U_0 is an energy scaling and nondimensionalizing parameter, and the strain energy is

$$U = (\sigma_x \epsilon_x + \sigma_y \epsilon_y + \tau_{xy}\gamma_{xy})/2 \tag{16}$$

in arbitrary x-y coordinates. (U is invariant in all coordinates.)

Up to this point, no difference exists between the present nonlinear version of the Ambartsumyan material model and the Jones-Nelson nonlinear weighted compliance matrix material model. Both models are based on eight independent nonlinear mechanical properties. The difference between the models arises when the compliance matrix in principal stress coordinates is formed. Then, the eight independent properties are used independently in the present modification of the Ambartsumyan model and are weighted in the Jones-Nelson model according to the proportions of tensile and compressive stresses. That is, the choices of the equivalent linear elastic properties are different for the two models. However, after those decisions are made in the manner of Eq. (2), the usual iteration procedure in Fig. 4 is followed, as described in the following paragraphs, for what amounts to a single element of a finite element approach to stress analysis, i.e., a uniform stress state.

Iteration Procedure

The first step in the iteration procedure is to determine the mechanical property vs strain energy relationships independently in tension and in compression from uniaxial stress-strain data. Thus, sets of constants A, B, C, and U_0 are determined for each independent mechanical property. Separate sets of constants are required for the tension and compression representation of a mechanical property variation with strain energy. (The number of independent properties required for an analysis is dependent on the body symmetry, the loading symmetry, and the degree of anisotropy of the material.)

The iteration procedure is started with the linear or "elastic" components of the tension material properties. (We could have, of course, started with the compression properties, but the choice is arbitrary.) The desired stresses and strains (including the principal stresses and corresponding nonprincipal strains) are calculated. Next, the principal stresses and their orientation are required for the multimodulus formulation. The strain energy then is calculated from the stresses and strains by use of one of the three strain energy approaches described in the next subsection.

New independent mechanical properties are determined after the strain energy is evaluated. This revised set of properties is used to form new all-tension and all-compression

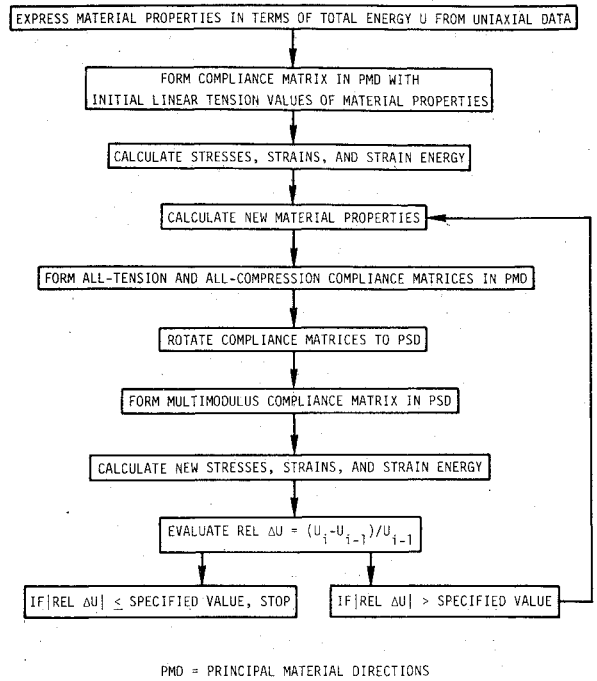

Fig. 4 Iteration procedure for nonlinear multimodulus materials.

compliance matrices in principal material directions. The compliance matrices of the tensile and compressive stress states then are transformed to principal stress directions. Next, the composition of the multimodulus compliance matrix is determined by use of the signs of the principal stresses in accordance with Eq. (2). The stresses and strains then are calculated by use of the compliance matrix or the stiffness matrix. However, one essential difference from usual stress analysis problems occurs: the calculation of stresses and strains is performed with a nonsymmetric compliance matrix and hence a nonsymmetric stiffness matrix. For this step, a nonsymmetric stiffness matrix equation solver such as that due to Cyr[18] is essential for calculation of stresses in nonuniform stress states. In uniform prescribed stress states, the determination of strains is a straightforward substitution process even though the stiffness matrix is nonsymmetric. In both types of stress states, the loop from the calculation of new material properties to the computation of stresses, strains, and strain energies is repeated until a convergence criterion is satisfied.

A convergence criterion based on the relative change in total strain energy is used in the nonlinear multimodulus material model. When the absolute value of the relative change in total strain energy, $|\text{rel}\ \Delta U|$, between two iterations $i-1$ and i

$$|\text{rel}\ \Delta U| = |(U_i - U_{i-1})/U_{i-1}| \tag{17}$$

is sufficiently small, then the iteration procedure is terminated, and convergence is defined for a single finite element or for a uniform stress state. In a finite element analysis, convergence is defined to occur when the foregoing convergence criterion is satisifed for every element.

Strain Energy Functions

Three different energy functions (total strain energy, divided strain energy, and weighted strain energy) are investigated for the nonlinear multimodulus material model. These strain energies are actually strain energy densities, but we abbreviate by dropping the word density.

In the total energy approach, all of the energy in Eq. (16) is used to determine the mechanical properties. This approach can be applied in any coordinate system because the strain energy is invariant under transformation of coordinates.

In the divided energy approach, the strain energy is separated into two components: 1) the contribution from tensile principal stresses, and 2) the contribution from compressive principal stresses. These two components are not invariant under rotation of coordinates and are defined only in principal stress coordinates. For example, if σ_p is tension and σ_q is compression, then

$$U_t = \tfrac{1}{2}\sigma_p\epsilon_p; \quad U_c = \tfrac{1}{2}\sigma_p\epsilon_q \tag{18}$$

The divided energy approach coincides with the total energy approach when the principal stresses are either all-tension or all-compression. In the material model, the tension component of strain energy, U_t, is used to determine tension mechanical properties, and the compression component of strain energy, U_c, is used to determine compression mechanical properties. This division of energy is a mechanism used to investigate the dependence of the relationship between strain energy and mechanical properties on the signs of the principal stresses.

In the weighted energy approach, the effective energy level in terms of the tension and compression components of the total strain energy is

$$U_w = (U_c^2 + U_t^2)/U \tag{19}$$

where U = total strain energy, U_c = compression strain energy, U_t = tension strain energy, and U_w = weighted strain energy. This weighted energy level is used to find both the tension and compression mechanical properties.

Strains predicted with the foregoing energy approaches in the nonlinear multimodulus model are compared with measured strains in the next section.

Comparison of Predicted and Measured Biaxial Strain Response

The biaxial strain response of hollow tubular ATJ-S graphite specimens measured by Jortner[12-14] is compared with predicted strain response in this section. The comparison is made to determine the influence of a symmetric vs a nonsymmetric compliance matrix on strain prediction. First, Jortner's strain measurements are described. Then, the various approaches to predict the strain response and to correlate it with the measured strain response are discussed.

Measured Strain Reponse

Jortner[12-14] measured axial and circumferential strains on the surface of hollow tubular specimens, as shown in Fig. 5 along with the strain gage locations. The specimen is subjected to internal pressure and either axial compression or axial tension loading. Hence, the specimen has circumferential tensile stresses and either axial compressive or axial tensile stresses. We restrict our attention to loadings that result in circumferential tensile and axial compressive stresses and, hence, excitation of multimodulus behavior.

Jortner's biaxial test specimen does not have a uniform stress state, even in the central region where the strains are measured. For example, a circumferential stress gradient exists through the thickness of the specimen. However, the gradient is small because the outer surface stress σ_θ is 0.96 times the mean circumferential stress.[14] Thus, when we want to determine the stresses at the location of the strain gages, we must adjust the average stresses reported by Jortner to account for the circumferential stress gradient. The axial strain gradient through the thickness (due to bending) is ignored because it is negligible.

The measured strains in specimens from two different ATJ-S graphite billets are listed for several loading conditions in Table 1. There, the nominal stress ratio is the ratio of the nominal or average applied axial stress to the average applied circumferential stress, $\sigma_z : \sigma_\theta$. The axial stresses are listed without adjustment from the actual nominal values. However, all circumferential stresses are 0.96 times the reported average stress to account for the aforementioned circumferential stress gradient. The strains are, of course, the actual measured values. These strains correspond to stresses that are well into the nonlinear range of the stress-strain curves measured by Jortner[14] and modeled by Jones and Nelson.[9,11]

Predicted Strain Response

The predicted strain response of the biaxial test specimens is based on the uniaxial stress-strain curves obtained by Jortner[14] for billet 16K9-27. That billet is the only billet for which a complete set of data is available for all properties ($E_{m_{tc}}$, $E_{n_{tc}}$, $\nu_{mn_{tc}}$, and $E^{45}_{mn_{tc}}$). The 16K9-27 billet data are used for predicted response of specimens made from both billet 16K9-27 and billet 1C0-15. We do not use the 16K9-27 data to predict the response of specimens from billet 1C0-15 accurately. That is, we are not trying to see how close the nonsymmetric or symmetric compliance matrix approaches with the various energy approches come to the absolute magnitudes of the measured strains. Instead, we merely seek the *relative* accuracy of each approach (relative to each other).

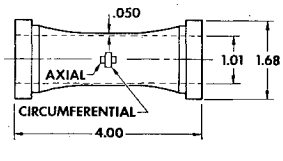

Fig. 5 Hollow graphite biaxial test specimen (dimensions in inches).

Table 1 Measured biaxial strains with corresponding applied stresses

Nominal stress ratio (σ_z: σ_θ)	Applied stresses at outer surface		Measured strains		Billet	Data source
	σ_z, psi	σ_θ, psi	ϵ_z	ϵ_θ		
−0.08:1	−400	4694[a]	−0.0008	0.0034	16K9-27	Ref. 12, Table IX
−0.64:1	−2250	3408	−0.00280	0.00304	1C0-15	Ref. 13, Fig. 66
−0.64:1	−2440	3706[a]	−0.0031	0.0034	1C0-15	Ref. 12, Table IX
−0.97:1	−3444	3408	−0.00465	0.00343	1C0-15	Ref. 14, Figs. 18 and 19
−0.99:1	−3515	3408	−0.00485	0.00343	1C0-15	Ref. 14, Figs. 18 and 19

[a] The specimen fractured at this stress level.

The uniaxial stress-strain curves in tension are shown, along with the Jones-Nelson nonlinear material model predictions, in Ref. 9. Similarly, the results in compression are shown in Ref. 11. Somewhat improved values of the corresponding Jones-Nelson model parameters are listed in Table 2. These parameters are used for both the weighted compliance matrix model[10] and the present nonsymmetric compliance matrix model.

The hollow tubular specimen in Fig. 5 has fairly predictable small stress gradients through its thickness. These known stress gradients will be used in conjunction with a nonlinear stress analysis of a uniformly stressed region to predict the strains on the surface of the central region of the tubular specimen. That is, the expense and effort of a finite element analysis are not needed to answer the basic question addressed in this paper. Instead, the central region of the tubular specimen is approximated as a uniformly stressed body (and the small stress gradients are ignored). The corresponding strain predictions are listed for the loading conditions of Table 1 in Table 3. There, the total, divided, and weighted energy approaches all are used for both the weighted compliance matrix model and the nonsymmetric compliance matrix model.

The predicted strains for the nonsymmetric compliance matrix model generally are somewhat better than those for the weighted compliance matrix model. This conclusion is valid for each energy approach and is based on deviations from measured strain values calculated from

$$\%\ \text{deviation} = \left[\frac{(\epsilon_{z_p}-\epsilon_{z_m})^2+(\epsilon_{\theta_p}-\epsilon_{\theta_m})^2}{\epsilon_{z_m}^2+\epsilon_{\theta_m}^2}\right]^{1/2}\times 100\% \qquad (20)$$

where

z = axial direction
θ = circumferential direction
m = measured value
p = predicted value

Table 2 Jones-Nelson nonlinear material model parameters for ATJ-S graphite billet 16K9-27[a]

Mechanical property	A	B	C	U_0, psi
E_{r_t}	2.40×10^6 psi	0.360	0.130	1
E_{z_t}	1.50×10^6 psi	0.307	0.182	1
$\nu_{r\theta_t}$	0.12	0.487	0.111	1
$\nu_{z\theta_t}$	0.14	0.346	0.229	1
$E^{45}_{rz_t}$	1.60×10^6 psi	0.234	0.239	1
E_{r_c}	1.80×10^6 psi	0.201	0.293	1
E_{z_c}	1.20×10^6 psi	0.166	0.327	1
$\nu_{r\theta_c}$	0.12	0.247	0.025	1
$\nu_{z\theta_c}$	0.095	0.005	0.965	1
$E^{45}_{rz_c}$	1.35×10^6 psi	0.166	0.323	1

[a] Experimental data due to Jortner,[14] Figs. 4, 5, 7, 9, 10, and 12.

Equation (20) is an error definition based on the length of the deviation vector in two-dimensional strain space relative to the length of the strain vector, as shown in Fig. 6.

We address the specific percentage deviations for the various energy approaches relative to whether the nonsymmetric or symmetric compliance matrix approach is adopted. For all loading conditions except the stress ratio −0.08:1, the percentage deviations for the nonsymmetric compliance matrix approach are from 2.6% to 0.2% lower than those for the symmetric compliance matrix approach. The only exception is for the stress ratio −0.08:1, where the nonsymmetric compliance matrix approach leads to strain predictions that are worse than those with the symmetric compliance matrix approach by up to 0.5%. Curiously, the poorest strain predictions are for specimens made from billet 16K9-27, from which the Jones-Nelson models are constructed. Data from billet 16K9-27 lead to better strain response predictions for billet 1C0-15 specimens than for specimens from billet 16K9-27. This somewhat anomalous behavior would be disturbing if our objective were to predict strain response accurately. However, we are only trying to determine whether compliance matrix asymmetry is important in strain predictions. Thus, we need only examine the inaccuracies in the various strain predictions in Table 3 relative to each other. Our conclusion is that compliance matrix asymmetry leads to negligible errors in calculation of strain response.

We could attempt to refine our predictions of strain response by developing the Jones-Nelson nonlinear material model for each approach from uniaxial tests on the Jortner biaxial specimen in Fig. 5 instead of on his uniaxial specimens. For example, Jones and Nelson[11] achieve better correlation of predicted and measured strain response for biaxial specimens when they use Jortner's uniaxial stress-strain data measured on the biaxial specimen. They also "adjust" data from uniaxial specimens (rods) to achieve "equivalent" biaxial specimen data. These types of refinements or adjustments could be made in the present work. However, the main point is that we can attribute only a negligible difference in predicted strain response to the asymmetry of the compliance matrix. Thus, we regard the refinements as an unnecessary step in our argument about the importance of including compliance matrix asymmetry in strain prediction calculations.

Concluding Remarks

The stress analysis of bodies made from materials with nonlinear stress-strain behavior under tension loading different from that under compression loading is re-examined. Specific attention is focused on the question of whether the compliance matrix, and hence the stiffness matrix, is inherently nonsymmetric, and what the consequences are in terms of stress or strain analysis. This question has widespread ramifications because, if multimodulus behavior is undeniably and strongly nonsymmetric, then most stress analysis techniques (except those relatively few already designed for nonsymmetric stiffness matrix problems) will have to be revised drastically. On the other hand, if multimodulus behavior can be approximated with a sym-

Table 3 Predicted biaxial strains for weighted compliance matrix and nonsymmetric compliance matrix nonlinear material models

Material model	Energy approach	Nominal stress ratio ($\sigma_z : \sigma_\theta$)	Predicted strains ϵ_z	Predicted strains ϵ_θ	Deviation, %
Weighted compliance matrix	Total	−0.08:1[a]	−0.00087	0.00378	11.1
		−0.64:1	−0.00314	0.00291	8.7
		−0.64:1[a]	−0.00351	0.00324	9.5
		−0.97:1	−0.00511	0.00324	8.5
		−0.99:1	−0.00524	0.00327	7.1
	Divided	−0.08:1[a]	−0.00072	0.00377	10.9
		−0.64:1	−0.00278	0.00273	7.4
		−0.64:1[a]	−0.00307	0.00303	8.2
		−0.97:1	−0.00461	0.00289	9.3
		−0.99:1	−0.00473	0.00290	9.1
	Weighted	−0.08:1[a]	−0.00087	0.00376	10.6
		−0.64:1	−0.00285	0.00270	8.3
		−0.64:1[a]	−0.00316	0.00299	9.0
		−0.97:1	−0.00448	0.00296	8.6
		−0.99:1	−0.00459	0.00298	8.7
Nonsymmetric compliance matrix	Total	−0.08:1[a]	−0.00085	0.00380	11.6
		−0.64:1	−0.00307	0.00298	6.7
		−0.64:1[a]	−0.00343	0.00332	7.3
		−0.97:1	−0.00498	0.00337	5.9
		−0.99:1	−0.00511	0.00339	4.5
	Divided	−0.08:1[a]	−0.00071	0.00378	11.1
		−0.64:1	−0.00274	0.00277	6.7
		−0.64:1[a]	−0.00302	0.00307	7.3
		−0.97:1	−0.00452	0.00297	8.3
		−0.99:1	−0.00464	0.00298	8.3
	Weighted	−0.08:1[a]	−0.00085	0.00378	11.1
		−0.64:1	−0.00282	0.00274	7.2
		−0.64:1[a]	−0.00311	0.00304	7.9
		−0.97:1	−0.00441	0.00303	8.1
		−0.99:1	−0.00451	0.00305	8.5

[a] The specimen fractured under these loading conditions.

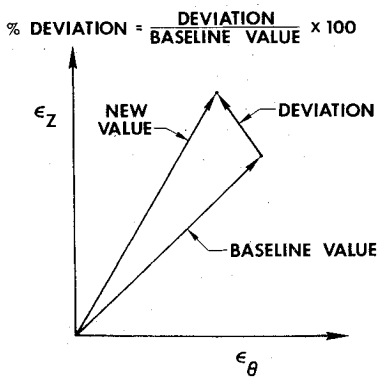

Fig. 6 Interpretation of percentage deviations in strains.

metric stiffness matrix, then many common stress analysis techniques can be modified easily for treatment of multimodulus materials.

Fortunately, the strain prediction inaccuracy ascribed solely to compliance matrix symmetry vs nonsymmetry is quite small. The accuracy improvement gained by considering compliance matrix nonsymmetry is at most 1% or 2% for a biaxially stressed ATJ-S graphite tubular body. For example, when compliance matrix nonsymmetry is ignored, the predicted strains are about 7-11% in error but are only 5-11% in error when nonsymmetry is accounted for. That is, no matter which energy approach (total, divided, or weighted) is used, the difference between a symmetric and a nonsymmetric compliance matrix approach is insignificant. Thus, compliance matrix nonsymmetry is but a small and essentially negligible part of the error in this complicated nonlinear multimodulus stress analysis problem. Accordingly, we can approximate multimodulus behavior confidently with symmetric compliance matrix approaches such as those due to Jones[1] and Jones and Nelson.[10]

Acknowledgment

This research was sponsored by the Air Force Office of Scientific Research/NA Grant 73-2532 and Lockheed Missiles and Space Company, Inc., Sunnyvale, Calif.

References

[1] Jones, R. M., "Stress-Strain Relations for Materials with Different Moduli in Tension and Compression," *AIAA Journal*, Vol. 15, Jan. 1977, pp. 16-23.

[2] Ambartsumyan, S. A., "The Axisymmetric Problem of a Circular Cylindrical Shell Made of Material with Different Stiffness in Tension and Compression," *Izvestiya Akademii Nauk SSR, Mekhanika*, No. 4, 1965, pp. 77-85; translation available from Scientific and Technical Aerospace Reports as N69-11070.

[3] Ambartsumyan, S. A., and Khachatryan, A. A., "Basic Equations in the Theory of Elasticity for Materials with Different Stiffness in Tension and Compression," *Inzhenernyi Zhurnal, Mekhanika Tverdogo Tela*, No. 2, 1966, pp. 44-53; translation available from The Aerospace Corp., El Segundo, Calif., as LRG-67-T-12.

[4] Ambartsumyan, S. A., "Equations of the Plane Problem of the Multimodulus Theory of Elasticity," *Izvestiya Akademii Nauk Armianskoi SSR, Mekhanika*, Vol. 19, No. 2, 1966, pp. 3-19; translation available from The Aerospace Corp., El Segundo, Calif.

[5] Ambartsumyan, S. A. and Khachatryan, A. A., "Theory of Multimodulus Elasticity," *Inzhenernyi Zhurnal, Mekhanika Tverdogo Tela*, No. 2, 1966, pp. 64-67; translation available from Scientific and Technical Aerospace Reports as N67-27610.

[6] Ambartsumyan, S. A., "Basic Equations and Relations in the Theory of Elasticity of Anisotropic Bodies with Differing Moduli in Tension and Compression," *Inzhenernyi Zhurnal, Mekhanika*

Tverdogo Tela, No. 3, 1969, pp. 51-61; translation available from The Aerospace Corp., El Segundo, Calif., as LRG-70-T-1.

[7] Isabekyan, N. G. and Khachatryan, A. A., "On the Multimodulus Theory of Elasticity of Anisotropic Bodies in a Plane Stress State," *Isvestiya Akademii Nauk Armianskoi SSR, Mekhanika*, Vol. 22, No. 5, 1969, pp. 25-34; translation available from R. M. Jones.

[8] Jones, R. M. and Nelson, D. A. R., Jr., "A New Material Model for the Nonlinear Biaxial Behavior of ATJ-S Graphite," *Journal of Composite Materials*, Vol. 9, Jan. 1975, pp. 10-27.

[9] Jones, R. M. and Nelson, D. A. R., Jr., "Further Characteristics of a Nonlinear Material Model for ATJ-S Graphite," *Journal of Composite Materials*, Vol. 9, July 1975, pp. 251-265.

[10] Jones, R. M. and Nelson, D. A. R., Jr., "Material Models for Nonlinear Deformation of Graphite," *AIAA Journal*, Vol. 14, June 1976, pp. 709-717.

[11] Jones, R. M. and Nelson, D. A. R., Jr., "Theoretical-Experimental Correlation of Material Models for Nonlinear Deformation of Graphite," *AIAA Journal*, Vol. 14, Oct. 1976, pp. 1427-1435.

[12] Jortner, J., "Multiaxial Behavior of ATJ-S Graphite, Interim Report," McDonnell-Douglas Astronautics Co.-West, Huntington Beach, Calif., Air Force Materials Lab. Technical Report AFML-TR-71-160, July 1971.

[13] Jortner, J., "Multiaxial Behavior of ATJ-S Graphite," McDonnell-Douglas Astronautics Co.-West, Huntington Beach, Calif., Air Force Materials Lab. Technical Report AFML-TR-71-253, Dec. 1971.

[14] Jortner, J., "Uniaxial and Biaxial Stress-Strain Data for ATJ-S Graphite at Room Temperature," McDonnell-Douglas Astronautics Co., Rept. MDC G3564, Huntington Beach, Calif., June 1972.

[15] Jones, R. M., *Mechanics of Composite Materials*, McGraw-Hill, New York, 1975, Chap. 2.

[16] Tsai, S. W., "A Test Method for the Determination of Shear Modulus and Shear Strength," Air Force Materials Lab. Technical Report AFML-TR-66-372, Jan. 1967.

[17] Gol'denblat, I. I. and Kopnov, V. A., "Strength of Glass-Reinforced Plastics in the Complex Stress State," *Polymer Mechanics*, Vol. 1, March-April 1965, pp. 54-59.

[18] Cyr, N. A., "Finite Element Analysis Using Nonlinear-Unsymmetric Material Constitutive Equations," Lockheed Missiles and Space Co., Rept. LMSC D516967, Sunnyvale, Calif., Feb. 1977.